

Article

Tertiary Waves Measured during 2017 Pohang Earthquake Using an Underwater Glider

Jung-Han Lee ^{1,2}, Sung-Hyub Ko ², Seom-Kyu Jung ² and Jong-Wu Hyeon ^{2,*}¹ Department of Electronic Engineering, Sogang University, Seoul 04107, Korea; leejunghan@kiost.ac.kr² Marine Security and Safety Research Center, Korea Institute of Ocean Science & Technology, Busan 49111, Korea; kosh@kiost.ac.kr (S.-H.K.); skjung@kiost.ac.kr (S.-K.J.)

* Correspondence: hyeon@kiost.ac.kr

Received: 18 August 2019; Accepted: 10 September 2019; Published: 14 September 2019



Abstract: An underwater glider equipped with a hydrophone observed the acoustic sounds of an earthquake that occurred on 15 November 2017 05:29:32 (UTC) in the Pohang area. The underwater glider observed the earthquake sounds after 19 s (05:29:51) at approximately 140 km from the Pohang epicenter. In order to distinguish the earthquake sound from the glider's operation noise, the noise sources and Sound Pressure Level (SPL) of the underwater glider were analyzed and measured at laboratory tank and sea. The earthquake acoustic signal was distinguished from glider's self-noises of fin, pumped Conductivity-Temperature-Depth profiler (CTD) and altimeter which exist over 100 Hz. The dominant frequencies of the earthquake acoustic signals due to the earthquake were 10 Hz. Frequencies at which the spectra had dropped 60 dB were 50 Hz. By analysis of time correlation with seismic waves detected by five seismic land stations and the earthquake acoustic signal, it is clearly shown that the seismic waves converted to Tertiary waves and then detected by the underwater glider. The results allow constraining the acoustic sound level of the earthquake and suggest that the glider provides an effective platform for enhancing the earth seismic observation systems and monitoring natural and anthropogenic ocean sounds.

Keywords: underwater glider; Pohang earthquake; tertiary waves (T-Waves); acoustic signal

1. Introduction

Seismic energy from submarine earthquakes is converted into acoustic energy at the seafloor-water boundary. A Tertiary wave (or T-wave) is the acoustic signal from these earthquakes. A T-wave typically has frequencies ranging from 4 to 50 Hz. T-waves propagate efficiently in the ocean compared to seismic waves through the earth and can be detected at great distances. Underwater sound observation techniques can directly observe oceanic earthquakes, landslides, volcanic eruptions, and corresponding underwater explosions in the ocean. Although not many, there have been some reports of direct observations of hydro-acoustic waves due to underwater seismic activity from an offshore observatory [1–4]. These are the first direct measurements ever performed in a tsunami generation area.

It is becoming increasingly important to acquire low-cost, high-efficiency, small-scale, unmanned, direct observation technology to replace existing high-cost, low-efficiency, large-scale, manned exploration platforms such as marine research vessels and stations in [1–6]. Unmanned observation platforms such as Argo floats, Underwater Gliders, WaveGliders, Autonomous Underwater Vehicles and Autonomous Surface Vehicles have been widely used in marine surveys and military defense operations. Among these platforms, underwater gliders have been actively used for measurement of environmental underwater ambient noise. The addition of a single hydrophone sensor to an underwater glider provides a capability for measurement of underwater noise level [7–14] and the addition of a hydrophone array enables surveillance of the underwater acoustic environment [15,16].

Research programs using these technologies have been conducted to investigate geophysical causes of seafloor earthquakes, landslides, volcanic eruptions and corresponding underwater explosions using hydrophone recorders [17,18], an underwater glider [19]. Reference [19] observed underwater sounds at depths of 200 to 600 m using an underwater glider at a distance of 10 km from the Lau Basin submarine volcano. The sound frequency due to the volcano was 10–300 Hz, and the sound level was –25 dB higher than the ambient noise level. The prototype and concept as ocean surface gateway (OSG) using WaverGliders for retransmitting data of ocean bottom package to shore were demonstrated in [20].

In this paper we report the analysis of earthquake sounds recorded by an underwater glider equipped with a single hydrophone during the magnitude 5.5 earthquake of 15 November 2017, at Pohang in the Republic of Korea. The underwater glider measured the earthquake sounds at about 140 km from the epicenter, in a water depth of about 200 m during an underwater noise measurement survey from Uljin to Geoseong along the east coast of South KOREA. In order to distinguish the earthquake sound from the glider's operation noise, the noise sources and Sound Pressure Level (SPL) of the underwater glider were analyzed and measured. Next, the earthquake sounds measured by the glider was analyzed in time and frequency domain. Finally, the time correlation of the seismic waves and earthquake sounds observed by the seismic land station and the glider were described.

2. Materials and Methods

2.1. Noise Sources of the Underwater Glider

Underwater gliders are propelled by adjusting the buoyancy, thereby using the resulting vertical motion to drive the glider. Underwater gliders have no propeller, so there is little operating noise. Its possible noise sources, such as the air bladder, fin steering, battery movement and volume piston are described in [21]. Chandrayadula et al. [11] showed that high-intensity sounds such as the sloshing of the glider at the sea surface, the bladder pump, the ballast pump, and the battery packs moving around are all broadband in nature. The bulk of the broadband noises were concentrated at the lower frequencies 0–3 kHz. However, these only describe possible noise sources and no specific frequency and noise-level analysis of each of the noise sources, including the driving and sensor component parts, has yet been studied. Recently, An analysis has been reported on the self-noise of only the driving part of the Petrel II underwater glider developed in China [22].

In this paper, the noise sources of the driving and sensor parts of the underwater glider observed the earthquake sounds are described in detail. A Slocum underwater glider (200 m class) manufactured by Teledyne-Webb Research is used in this study (Figure 1). The glider has an overall length of 1.5 m and a mass of 60 kg. The buoyancy engine is an electrically powered piston drive, located in the nose section of the glider. The drive allows the glider to take in and expel water, thereby changing its overall buoyancy. The mechanism allows a nearly neutrally buoyant trimmed glider to change its displacement in water by ± 250 cc which corresponds to approximately $\pm 0.5\%$ of the total volume displaced. This change in buoyancy generates a vertical force which is translated through two swept wings into a combined forward and up/downward motion. Due to the location of the piston drive, also called the buoyancy engine, the change in direction of the buoyant force also creates the main pitching moment for the glider. Besides the buoyancy engine the glider possesses two more control actuators, a 9.1 kg battery pack, referred to as the sliding mass, that can be linearly translated along the main axis of the glider and a rudder attached to the vehicle tail fin structure. The sliding mass is used for fine tuning the pitch angle. A pumped Conductivity-Temperature-Depth profiler (CTD) sensor is contained in the payload bay of the glider. When the underwater glider moves vertically and horizontally, the driving and sensor parts generate noise. The noise sources associated with the driving parts include a piston, pitch controller, fin, and air bladder. The sensor noise sources are a pumped CTD and an altimeter.

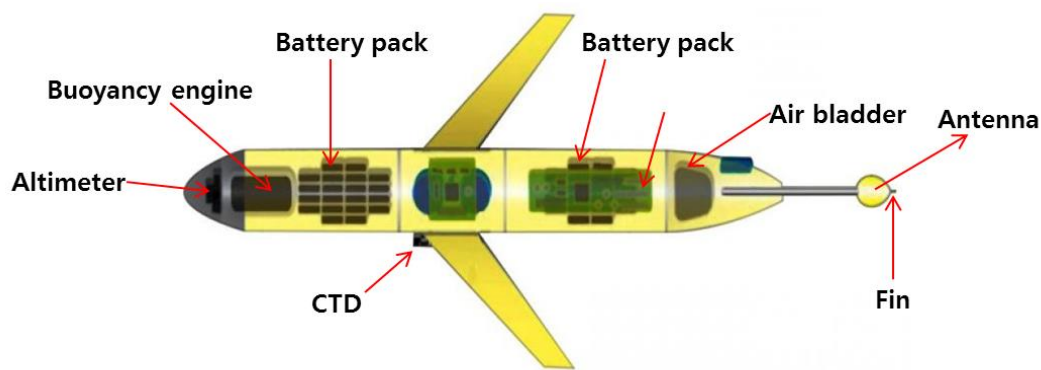


Figure 1. Components of the Slocum Underwater Glider.

2.2. Driving-Part Noise Sources

To change its direction of vertical motion the underwater glider piston pulls sea water to change the effective hull volume. This produces a combined noise from the dc motor, reducer, ball screw (linear motion) and piston. When the glider's vertical motion changes, the glider moves the battery pack back and forth to adjust the angle of the bow to match the hull glide angle. This produces a combined noise of dc motor, reducer, lead screw and battery pack sliding. The underwater glider moves the tail fin to control the direction of movement every 3 to 4 s. This generates a noise from a small stepper-motor drive. An air bladder operating under the tail antenna prevents the tail antenna from sinking into the water when the underwater glider is surfacing for Iridium communication. An air pump drive starts as the glider ascends through the uppermost 10 m water depth; this pump generates noise.

2.3. Sensor-Part Noise Sources

For stable CTD measurement, water is pumped through the CTD sensor and this generates noise. The pumped CTD operates continuously. The rate of pumping can be changed according to whether the glider is descending or ascending. The altimeter is normally used only while diving to prevent the glider from hitting the sea floor. This is yet another source of noise.

3. Results

3.1. Noise Measurement of the Underwater Glider

3.1.1. Glider's Operation Noise Measurement at Laboratory Tank

Sound pressure level (SPL) is usually expressed as twenty times the logarithm to base 10 of the ratio of the root-mean-square sound pressure to the reference sound pressure: $SPL = 20 \log (\hat{p}/p_0)$ where \hat{p} and p_0 are the root-mean-square sound pressure and reference sound pressure, respectively. SPL has units of dB re $1 \mu\text{Pa}^2$. SPL values of the driving- and sensor-part noise sources are discussed.

Noises from both the driving and sensor parts of the underwater glider were measured in a laboratory tank (Figure 2). The size of the tank is 20 m (W) \times 50 m (L) \times 10 m (D) and water depth in the tank was about 8 m. Since the water tank contained fresh water, the buoyancy of the underwater glider was adjusted in advance to be neutrally buoyant in fresh water. In order to record the noise of the underwater glider, a hydrophone was mounted on the underwater glider body. The reference value was $-168 \text{ dB re } 1 \mu\text{Pa}^2$. The gain and resolution of the recorder were 30 dB and 16 bits, respectively.

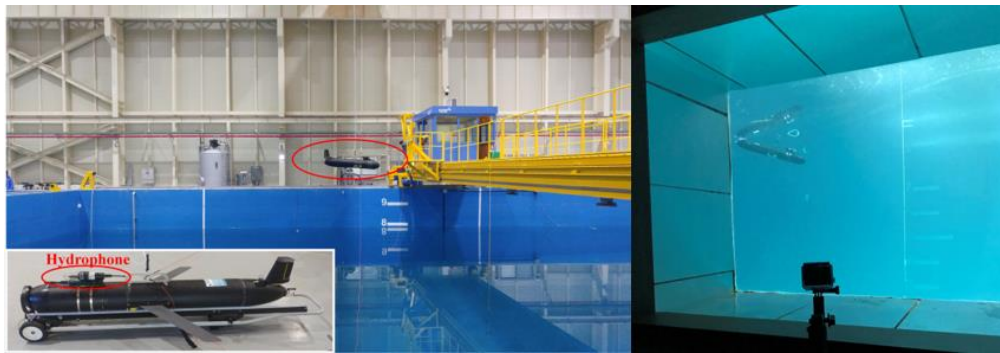


Figure 2. A underwater glider being prepared for immersion into a tank and diving.

Except for the tail, which was used for radio frequency communication with the operator, the underwater glider was fully submerged. Noise was generated by inputting an operation command arbitrarily to measure the SPL of each driving and sensor component (Figure 3). Fin noise measurement, however, was not possible because the tail was not submerged, to allow for radio frequency communication. The noise analysis of fin operation was obtained from the recorded data at sea, as described in the next section. The pumped CTD did not work due to the low electrical conductivity value of the fresh water used in the tank; so, the pumped CTD noise analysis is also described in the next section. The Piston noise level spectrum rises above the background level by more than 5 dB in all frequency bands up to 10 kHz (Figure 4a). The Pitch noise level likewise rises by more than 5 dB in frequency bands above 1 kHz (Figure 4b). The Air bladder noise level rises more than 10 dB at 155, 310, 463, 522, 552, 618 Hz and to a lesser extent in a broad frequency band (Figure 4c). The Altimeter noise level rises more than 5 dB at frequencies above 100 Hz (Figure 4d). To record noise from the flow between the underwater glider and the hydrophone, the glider performed a “yo” (descent and ascent) mission. By measuring the noise from repeated yo missions, it was confirmed that there was no flow noise caused by turbulence between the underwater glider body and the hydrophone.

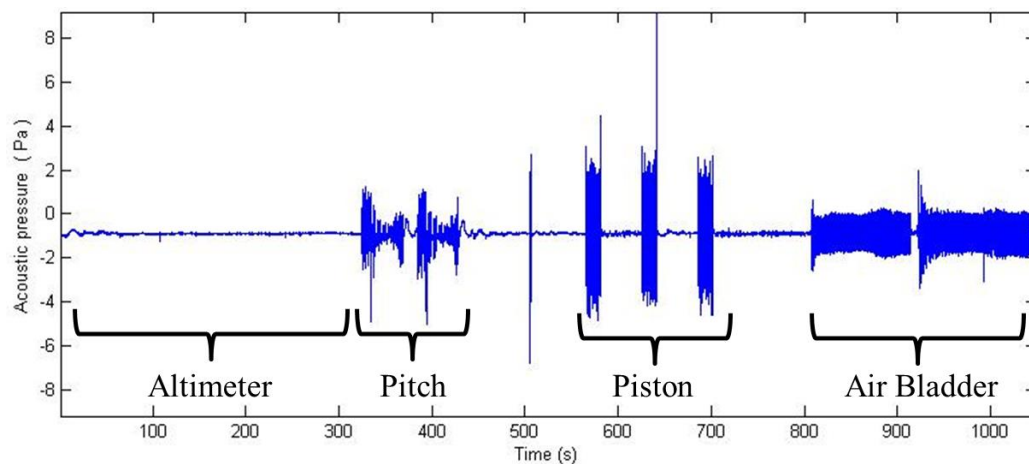


Figure 3. Recorded noise signal when the underwater glider operates in the laboratory tank.

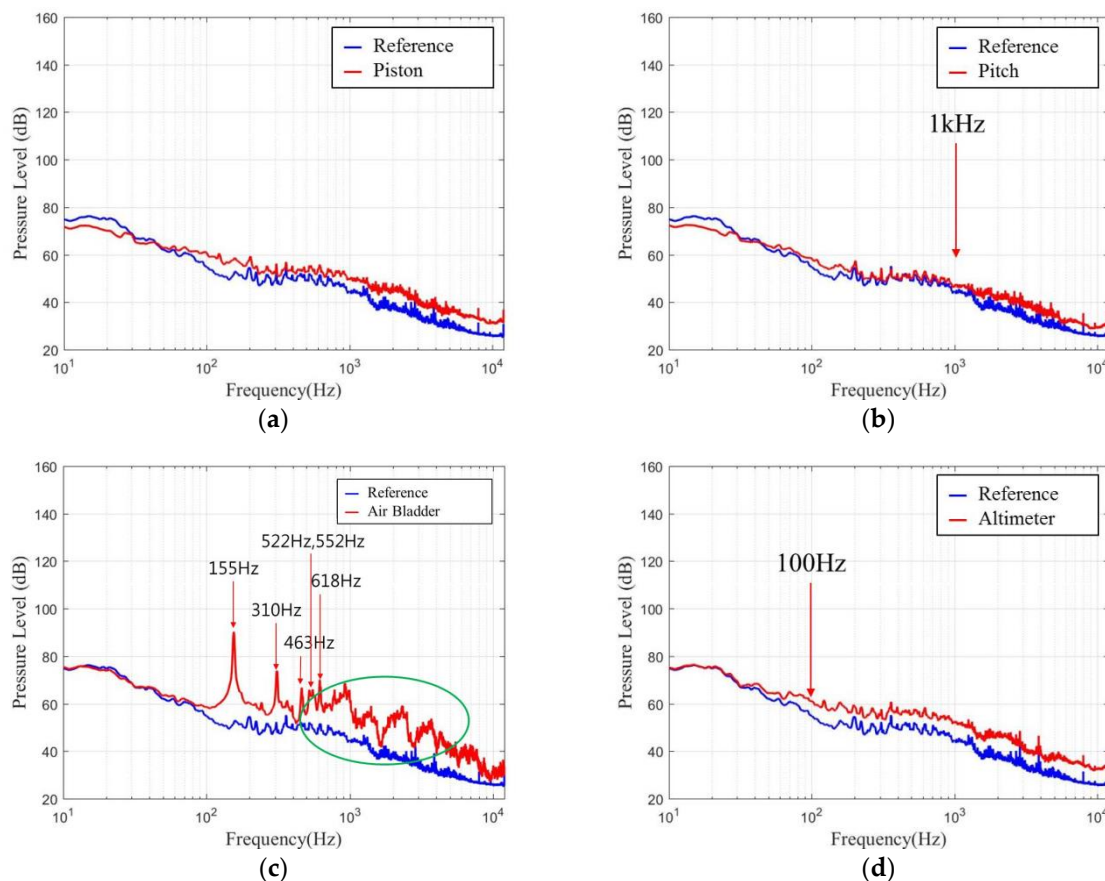


Figure 4. Measurement noise level when the underwater glider operates in the laboratory tank: (a) Piston, (b) Pitch, (c) Air Bladder, and (d) Altimeter.

3.1.2. Glider's Operation Noise Measurement at Sea

The underwater glider dived to a depth of 10–200 m and repeated six yo missions during about 6 h. It took about one hour for each yo. Figure 5 shows the command values of the driving part according to the water depth when the underwater glider is operated at sea. The driving-unit command value is −1 (low) to +1 (high).

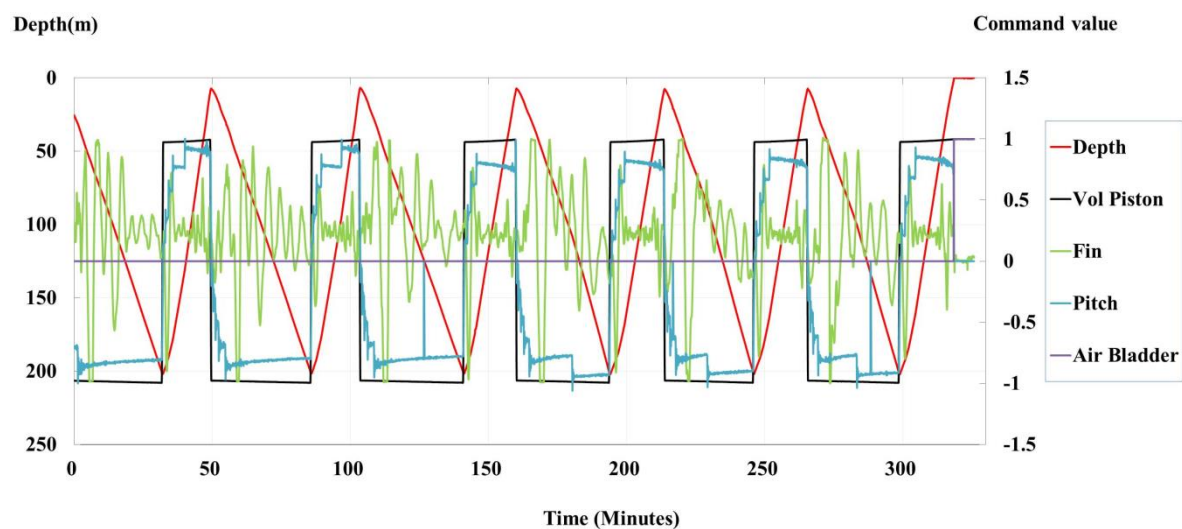


Figure 5. Command values when the glider is operating at sea.

When the underwater glider changes from descent to ascent, the values of the buoyancy control (Vol Piston) and the Pitch control (Pitch) change from -1 to $+1$; these values are negative during descent and positive during ascent. The Fin controller operated once every 3 to 4 s and the command value changed fast, regardless of descent or ascent. It can be seen that the Air Bladder command value is 0 except near the end when it is 1 as the bladder inflates raising the glider to the surface thereby allowing communication with the operator via satellite.

The Fin and pumped CTD noise levels were calculated from recorded data at sea. The same hydrophone was mounted on the same position of the underwater glider body as at tank experiment. Due to the ambient noise contained in the recordings at sea, the reference sound level of Fin and pumped CTD is greater than that in the laboratory tank. The Fin noise level rose 4–5 dB at frequencies of 800–950 Hz (Figure 6a). The pumped CTD noise level rose by more than 10 dB at discrete frequencies of 357, 410, 710, and 1450 Hz (Figure 6b).

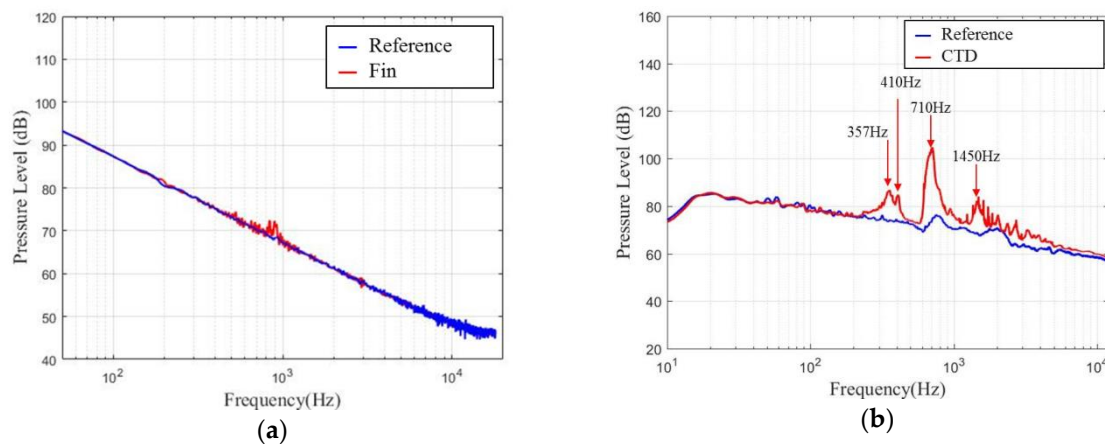


Figure 6. Measurement noise levels during underwater glider operation at sea: (a) Fin, and (b) Pumped Conductivity-Temperature-Depth profiler (CTD).

3.2. Pohang 2017 Earthquake: Analysis of in Situ Observations

3.2.1. In Situ Underwater Ambient Noise Measurement

The measurement survey of underwater ambient noise was conducted using an underwater glider with a single hydrophone from 13 to 17 November 2017 from Uljin to the Goseong area, along the east coast of South Korea in Figure 7. The underwater glider was launched at Uljin 13 November 05:04 (UTC) and recovered at Goseong 17 November 06:20 (UTC) using the R/V Eodo of Korea Institute Ocean Science and Technology. The underwater glider moved vertically between depths of about 10 m and 200 m. During the survey, the glider advanced at an average horizontal speed of 0.02 m/s, logging data while repeatedly taking profiles between 10 and 200 m depth. The glider drifted when it surfaced between dives to transmit CTD data and Global Positioning System (GPS) data to the shore station through a satellite connection. The average surface current calculated from the glider's GPS data was northward with a velocity of 0.35 m/s.

A single omni-directional hydrophone (HTI92MIN from High Tech with a sensitivity of -168 dB re $1\text{V}/1\mu\text{Pa}$) was mounted on the underwater glider. We synchronized the time of the hydrophone with the underwater glider before launched the glider. The signal was digitized by the internal acoustic data logger at a 24 kHz sample rate with 16-bit resolution and 30 dB gain. Each file was approximately 255 MB in size, 60 min long; a total of 18.3 GB was stored on the 128 GB internal flash memory during the 4-day survey. No acoustic data were transmitted in real time due to the large size of the files. All recorded data were processed using MATLAB software after the recovery of the glider. Recordings from the survey produced a one-dimensional time series of sound level spanning approximately 150 km from Uljin to Geseong. During the survey, on 15 November 05:29:32 (UTC), a magnitude

5.5 earthquake occurred at Pohang (epicenter 36.12°N, 129.36°E) [23,24]. Underwater sounds resulting from the momentary earthquake were observed in the glider's acoustic record.

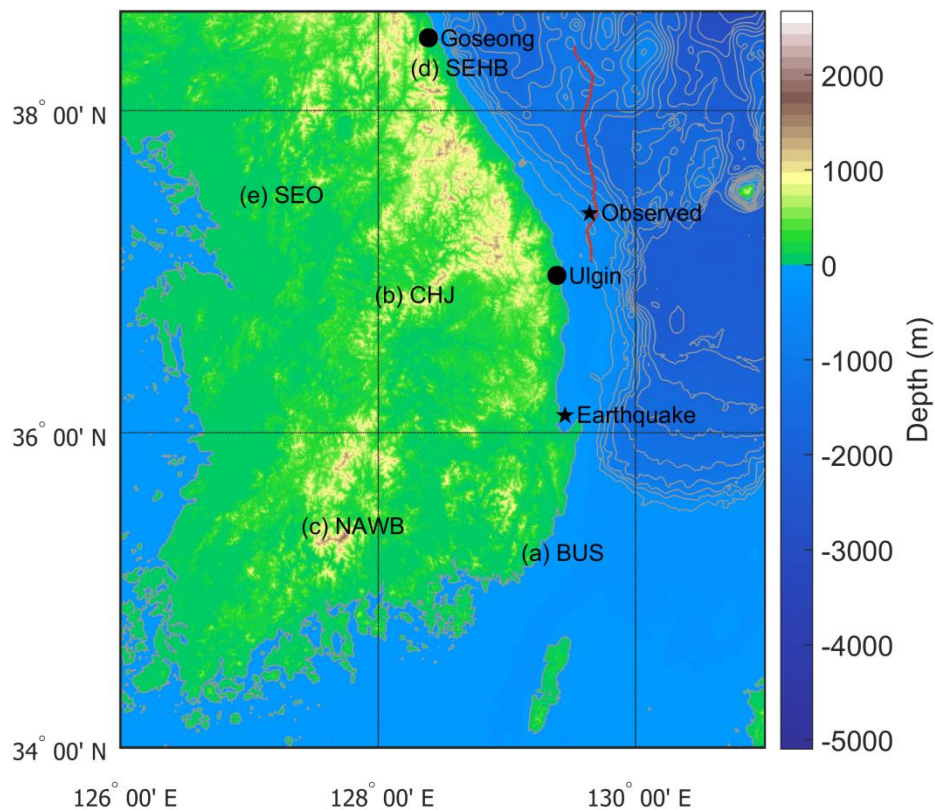


Figure 7. Underwater glider survey track (red line) map (seismic station: (a) Busan (BUS), (b) Chungju (CHJ), (c) Namwon (NAWB), (d) Seawha (SEHB), (e) Seoul (SEO)).

3.2.2. Underwater Position of Underwater Glider

The glider surfaced every 5 h and sent the GPS location information during the survey. The underwater trajectory of the glider was calculated by a linear interpolation between every two surfaced GPS points. When the earthquake occurred at 05:29:32 (UTC), the surfaced GPS positions were 37.3482°N, 129.6948°E at 00:55:19 (UTC) and 37.3806°N, 129.6994°E at 05:52:46 (UTC), respectively. The calculated GPS position of the glider is at 37.378°N, 129.699°E, approximately 140 km from the Pohang epicenter when the glider recorded acoustic sounds from the earthquake at 05:29:51 (UTC). The depth of the seafloor bottom and the glider at the GPS position was at about 430 m and 200 m, respectively.

3.2.3. Time and Frequency Analysis of Earthquake Underwater Sound

It is most common for noise signals to be represented in the frequency domain as noise spectral levels plotted as a function of frequency [25,26]. The data for ambient noise is usually expressed as spectral density (SD) levels or power spectral density (PSD), where the data in each frequency band has been normalized by dividing by the bandwidth of the frequency band. The units of the levels in each band are then dB re 1 $\mu\text{Pa}^2/\text{Hz}$. We used the following analysis method to distinguish earthquake underwater sounds. Extraction of necessary timing data from the recording files; Calculation of Power Spectrum Density (PSD) using a time window of chosen length in each recording. The length and overlap of FFT window for 1s and 50 %, respectively; Correction of PSD for recorder's sensitivity, gain and, when possible, frequency response to get the output data in sound pressure units (μPa).

Figure 8 shows PSD of a 1 h recording started at 05:29:35 (UTC) collected by the glider when the earthquake occurred at 05:29:32 (UTC). It contains underwater earthquake sound as well as the

operating noise of the glider's machinery mentioned in Section 3, e.g., piston and pitch motors, fin, airbladder, altimeter, pumped CTD. The glider descended with pumped CTD and altimeter turned on until it reached the turning depth (200 m), and it then turned on the piston and pitch motor for ascending and inflated the external air bladder to begin surfacing for communication. The pumped CTD and altimeter were turned off when the glider was ascending. The earthquake sounds were dominated below about 50 Hz.

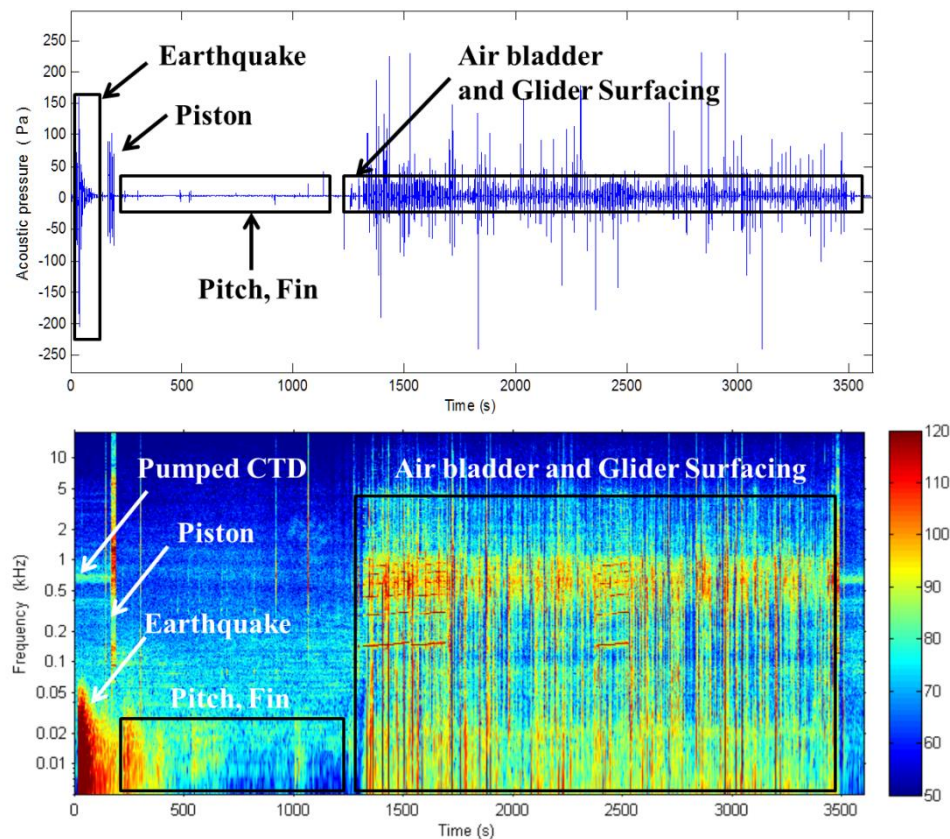


Figure 8. Spectrogram of earthquake underwater sound recording (started at 05:29:35 UTC).

The time sequence of the acoustic signal has been reconstructed, from the wav-file records starting at 05:29:35 (UTC) in Figure 9a. This time is the start reference time $t_0 = 0$ s (i.e., when the recording starts at 05:29:35); 16 s later (i.e., $t_1 = 05:29:51$), is the time of first arrival of the earthquake sounds at the glider's position, at about 200m depth. The arrival time (t_1) at about 19 s from earthquake correspond to about 7 km/s which may be the speed of seismic waves in the crust just up to the bottom of detection point, then in the water column and finally detected by the underwater glider. These sounds were observed for over 30 s.

Spectrum and spectrogram analyses of the earthquake sound have been carried out. By carefully examining the frequency spectrum of the record in Figure 9b, it can be seen that the dominant frequency of the earthquake sounds was about 10 Hz. Figure 9c shows that after the earthquake occurred, the average ambient noise level at frequencies below 50 Hz was approximately 60 dB higher than the ambient noise level before the earthquake occurred. The earthquake acoustic signal can be distinguished from glider's self-noises of fin, pumped CTD and altimeter. The fin noise exists at frequencies of 800–950 Hz every 3 to 4 s. The pumped CTD sensor noise exists at discrete frequencies of 357, 410, 710, 1450 Hz. The dominant CTD noise frequency is 710 Hz. The altimeter noise exists at frequencies above 100 Hz.

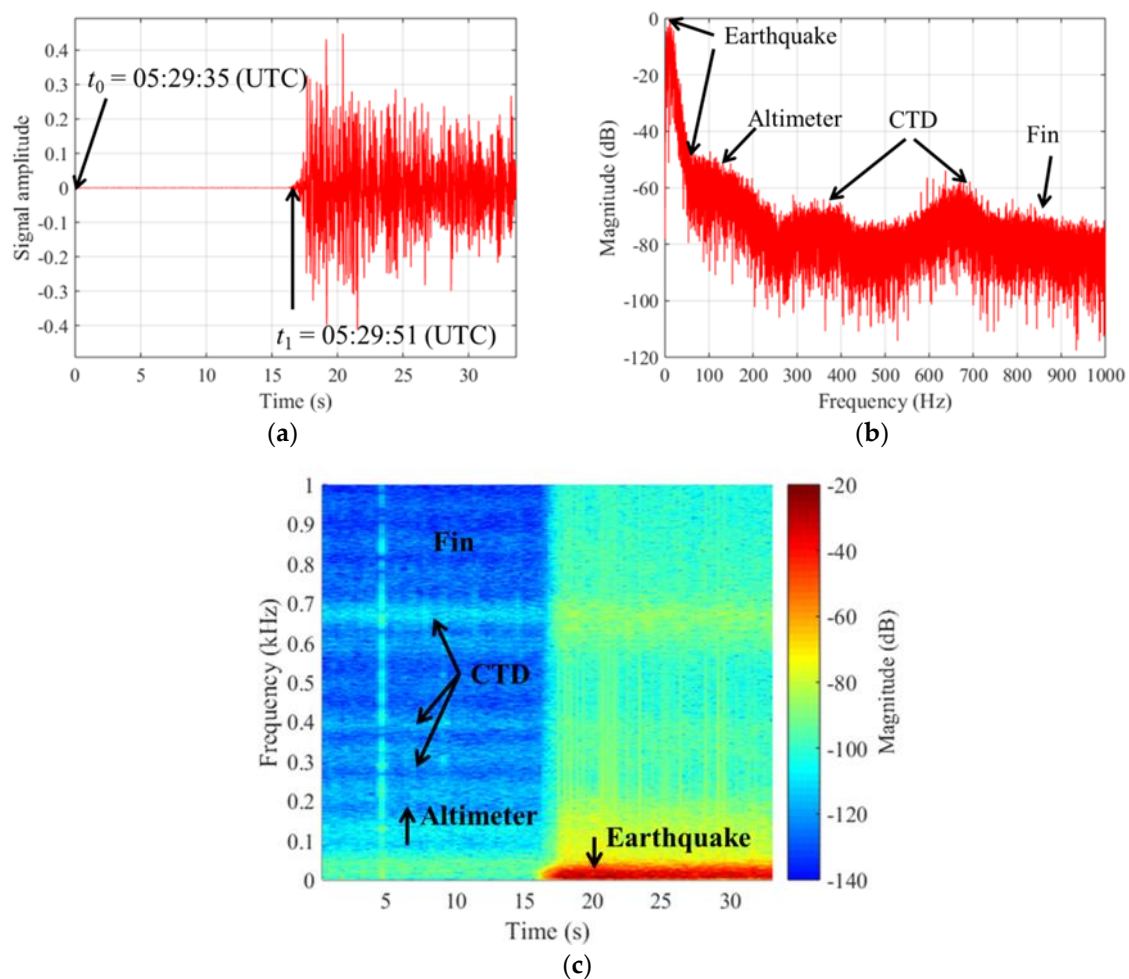


Figure 9. The earthquake acoustic signal: (a) Time reconstructed signal, (b) frequency spectrum and (c) Spectrogram.

3.2.4. Correlation with Situ Seismic Waves and Earthquake Sounds

Earthquake generated acoustic waves in the ocean are referred to as T-wave because in certain conditions, when they reach the shore, they may convert back to seismic waves and arrive third after the P- and S-seismic waves on near-shore seismological stations.

IRIS (Incorporated Research Institutions for Seismology) archives waveform (time-series) data from stations around the world. Seismic wave data of the Pohang Mw 5.5 earthquake was collected by the Busan (35.25°N, 129.11°E), Chungju (36.87°N, 127.97°E), Namwon (35.42°N, 127.40°E), Seawha (38.27°N, 128.25°E), Seoul (37.49°N, 126.92°E) station in Figure 7. The Busan (BUS) station was about 92 km away from the Pohang epicenter; the Chungju (CHJ) station was 147 km, Namwon (NAWB) station was 183 km, Seawha (SEHB) station and Seoul (SEO) station were 255 km same distance. The underwater glider was about 140 km away from the Pohang epicenter.

The time series of the seismic and earthquake acoustic signal detected at the five stations and the underwater glider are presented in Figure 10. The time of arrival of the seismic waves observed at the station is proportional to the distance from the epicenter. Since the underwater glider was closer than Chungju station to the epicenter, the arrival time of the T-wave (i.e., earthquake acoustic signal) observed by the underwater glider was earlier than that of the seismic waves observed at the Chungju station. The seismic P- and S-waves travel at velocities from 2000 to 7000 m/s in the crust just up to the seafloor bottom (about 430 m) of detection point, then in the water column and finally detected by the underwater glider (about 200 m). It is clearly shown that the acoustic signal detected by the glider from the Pohang earthquake is a Tertiary wave (T-wave) in Figure 11.

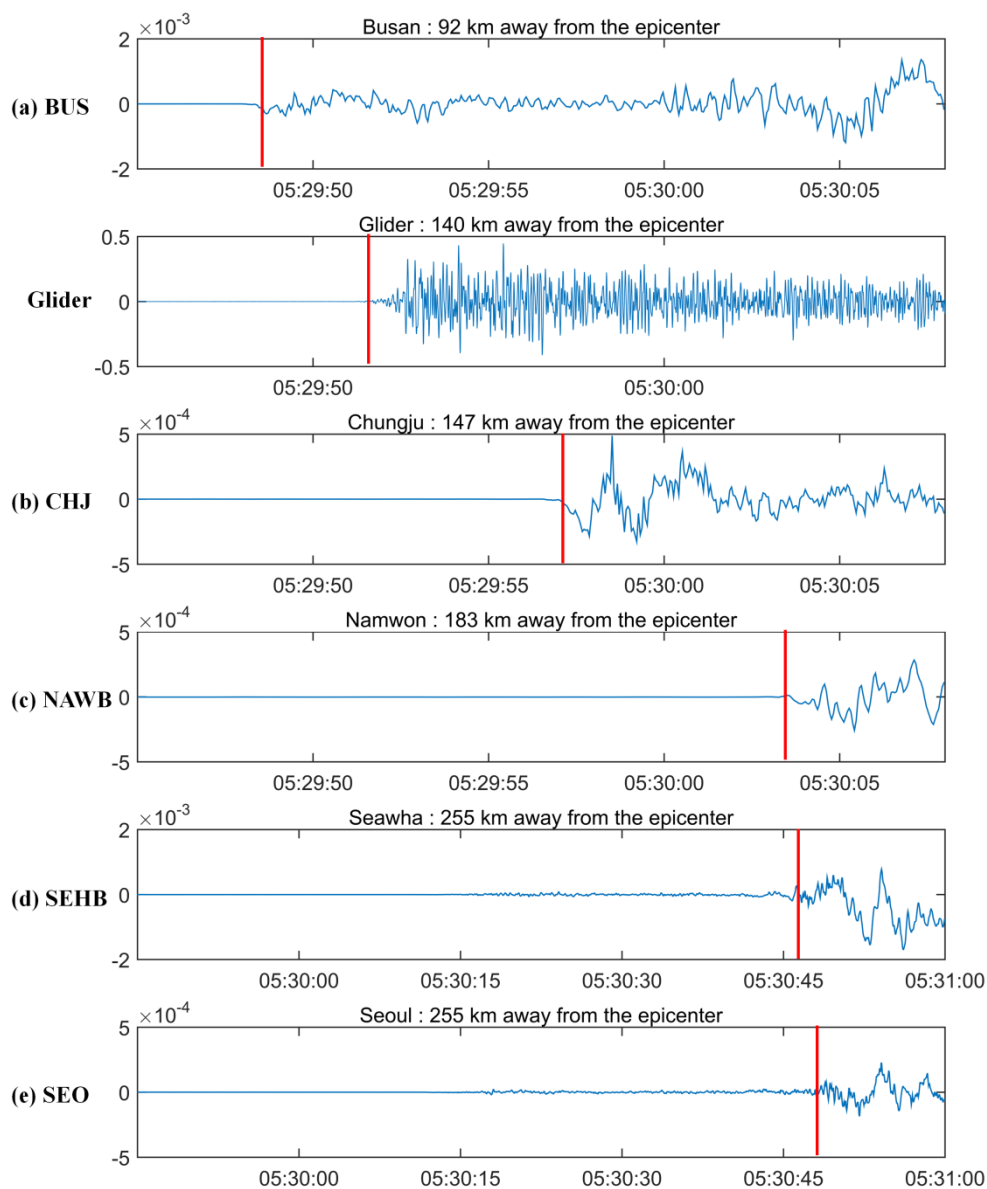


Figure 10. Time signal of the seismic and T-waves observed by the seismic observatory and underwater glider position from the Pohang earthquake epicenter.

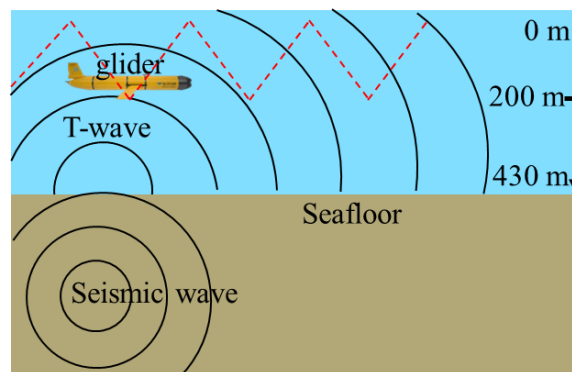


Figure 11. The creation of T-waves from seismic waves and detection by the underwater glider.

4. Discussion

Early models of the Slocum underwater glider were equipped with a non-pumped CTD. The non-pumped CTD has a large salinity uncertainty because the flow rate in the conductivity cell is not constant. The salinity measurement uncertainty of a non-pumped CTD was about 30 times greater than that of a pumped CTD [27]. To obtain good quality ocean observation data, recently-produced Slocum underwater gliders are equipped only with a pumped CTD. In terms of the overall operating time of the underwater glider, the pumped CTD noise is higher and it occurs for a longer time than noise from other sources. It is the main noise source in underwater glider operation.

When an acoustic source emits in a test tank, acoustic waves are reflected by the walls, the surface, and the bottom. The multiple reflections give rise to a reverberated field. Measuring underwater sound power in reverberant environment such as a tank has advantages of speed but is limited in accuracy and frequency range, but it has been used to good effect in specific applications. For small sources (or small noisy components) like underwater glider, it is possible to make measurements of radiated noise in reverberant tanks [28].

For the seismic observation of seafloor and coastal earthquake disaster risk assessment, a comprehensive analysis of seismic sources is needed. This requires simultaneously observing underwater phenomena caused by seafloor earthquakes. Moreover, submarine earthquake underwater acoustical observation technology using underwater gliders is very synergistic because it can provide basic research data on natural, anthropogenic, and ecological underwater sources in the ocean. In addition, underwater sound observations using underwater gliders can be of great assistance in developing earth observation systems by providing submarine platforms ensuring stable operational technology and linking with existing earthquake observation networks.

To this end, improving the method for estimating a glider's underwater trajectory is important because it is a challenging task due to several errors in the linear interpolation method. It is not realistic because the position is estimated by dividing the distance between the real GPS fixed position by transit time, and the glider's direction and speed remain constant. In other words, the trajectory looks like a straight line. Our future work aims to provide a better method for estimating a glider's optimal underwater trajectory, focusing on the importance of the ocean currents and underwater wireless communication technology to transmit the acoustic data observed by the underwater glider to the shore in real time through the OSG such as WaveGliders in [20].

5. Conclusions

In this study, the acoustic sounds of earthquake occurred on 15 November 2017 in the Pohang area of South Korea observed by underwater glider were analyzed. By analysis of time correlation with seismic waves detected by five seismic land stations and the earthquake acoustic signal, it is clearly shown that the seismic waves converted to Tertiary waves (i.e., earthquake acoustic signal) and then it detected by the underwater glider. In order to distinguish the earthquake sound from the glider's operation noise, Sound Pressure Level (SPL) of the noise sources associated with the driving and sensor parts of the underwater glider were analyzed and measured at laboratory tank and sea. The earthquake acoustic signal in the range of 10–50 Hz was distinguished from glider's self-noises which are exist over 100 Hz. The results allow constraining the acoustic sound level of the earthquake and suggest that the glider provides an effective platform for enhancing the earth seismic observation systems and monitoring natural and anthropogenic ocean sounds.

Author Contributions: Conceptualization, methodology, investigation, writing—original draft preparation, writing—review and editing, J.-H.L., S.-H.K. and J.-W.H.; project administration, S.-K.J.

Funding: This research was funded by Korea Institute of Ocean Science & Technology, grant number PE99741.

Acknowledgments: This research was part of the project titled “Development of maritime defense and security technology [PE99741]” funded by Korea Institute of Ocean Science & Technology in 2019.

Conflicts of Interest: The authors declare no conflict of interest.

References

1. Momma, H.; Fujiwara, N.; Kawaguchi, K.; Iwase, R.; Suzuki, S.; Kinoshita, H. Monitoring system for submarine earthquakes and deep sea environment. In Proceedings of the OCEANS'97. MTS/IEEE Conference Proceedings, Halifax, NS, Canada, 6–9 October 1997; pp. 1453–1459.
2. Baba, T.; Hirata, K.; Kaneda, Y. Tsunami magnitudes determined from ocean-bottom pressure gauge data around Japan. *Geophys. Res. Lett.* **2004**, *31*. [[CrossRef](#)]
3. Nosov, M.; Kolesov, S.; Denisova, A.; Alekseev, A.; Levin, B. On the near-bottom pressure variations in the region of the 2003 Tokachi-Oki tsunami source. *Oceanology* **2007**, *47*, 26–32. [[CrossRef](#)]
4. Bolshakova, A.; Inoue, S.; Kolesov, S.; Matsumoto, H.; Nosov, M.; Ohmachi, T. Hydroacoustic effects in the 2003 Tokachi-oki tsunami source. *Russ. J. Earth Sci.* **2011**, *12*, 1–14. [[CrossRef](#)]
5. Cecioni, C.; Romano, A.; Bellotti, G.; De Girolamo, P. Hydroacoustic waves measured during the 2012 Negros-Cebu earthquake. *J. Waterw. Port Coast. Ocean Eng.* **2018**, *144*. [[CrossRef](#)]
6. Abdolali, A.; Cecioni, C.; Bellotti, G.; Kirby, J.T. Hydro-acoustic and tsunami waves generated by the 2012 Haida Gwaii earthquake: Modeling and in situ measurements. *J. Geophys. Res. Oceans* **2015**, *120*, 958–971. [[CrossRef](#)]
7. Holmes, J.D.; Carey, W.M.; Lynch, J.F. An overview of unmanned underwater vehicle noise in the low to mid frequencies bands. *Proc. Meet. Acoust.* **2010**, *9*. [[CrossRef](#)]
8. Silva, A.; Matos, A.; Soares, C.; Alves, J.C.; Valente, J.; Zabel, F.; Cabral, H.; Abreu, N.; Cruz, N.; Almeida, R. Measuring underwater noise with high endurance surface and underwater autonomous vehicles. In Proceedings of the 2013 OCEANS-San Diego, San Diego, CA, USA, 23–26 September 2013; pp. 1–6.
9. Jiang, Y.-M.; Alvarez, A.; Cecchi, D.; Garau, B.; Micheli, M. In-situ acoustic received level measurements with glider based reactive behaviour. In Proceedings of the OCEANS 2015-Genova, Genova, Italy, 18–21 May 2015; pp. 1–6.
10. Takahashi, R.; Akamatsu, T.; Hasegawa, D.; Okunishi, T.; Nishida, Y.; Ura, T.; Takahashi, H.; Katsuragawa, M. Evaluation of availability on passive acoustic devices on underwater platforms. In Proceedings of the 2016 Techno-Ocean (Techno-Ocean), Kobe, Japan, 6–8 October 2016; pp. 317–320.
11. Chandrayadula, T.K.; Miller, C.W.; Joseph, J. Monterey Bay ambient noise profiles using underwater gliders. *J. Acoust. Soc. Am.* **2013**, *133*, 3395. [[CrossRef](#)]
12. Cauchy, P.; Testor, P.; Mortier, L.; Beguery, L.; Bouin, M.-N. Passive acoustics embedded on gliders—Weather observation through ambient noise. *J. Acoust. Soc. Am.* **2014**, *135*, 2306–2307. [[CrossRef](#)]
13. Ferguson, B.G.; Lo, K.W.; Rodgers, J.D. Sensing the underwater acoustic environment with a single hydrophone onboard an undersea glider. In Proceedings of the OCEANS 2010 IEEE-Sydney, Sydney, Australia, 24–27 May 2010; pp. 1–5.
14. Maguer, A.; Dymond, R.; Grati, A.; Stoner, R.; Guerrini, P.; Troiano, L.; Alvarez, A. Ocean gliders payloads for persistent maritime surveillance and monitoring. In Proceedings of the 2013 OCEANS-San Diego, San Diego, CA, USA, 23–26 September 2013; pp. 1–8.
15. Nielsen, P.L.; Siderius, M.; Muzi, L. Glider-based seabed characterization using natural-made ambient noise. In Proceedings of the OCEANS 2015-Genova, Genova, Italy, 18–21 May 2015; pp. 1–7.
16. Tesei, A.; Been, R.; Williams, D.; Cardeira, B.; Galletti, D.; Cecchi, D.; Garau, B.; Maguer, A. Passive acoustic surveillance of surface vessels using tridimensional array on an underwater glider. In Proceedings of the OCEANS 2015-Genova, Genova, Italy, 18–21 May 2015; pp. 1–8.
17. Roth, E.H.; Hildebrand, J.A.; Wiggins, S.M.; Ross, D. Underwater ambient noise on the Chukchi Sea continental slope from 2006–2009. *J. Acoust. Soc. Am.* **2012**, *131*, 104–110. [[CrossRef](#)] [[PubMed](#)]
18. Spindel, R.C.; Na, J.; Dahl, P.H.; Oh, S.; Eggen, C.; Kim, Y.G.; Akulichev, V.A.; Morgunov, Y.N. Acoustic tomography for monitoring the Sea of Japan: A pilot experiment. *IEEE J. Ocean. Eng.* **2003**, *28*, 297–302. [[CrossRef](#)]
19. Matsumoto, H.; Stalin, S.; Embley, R.; Haxel, J.; Bohnenstiehl, D.; Dziak, R.; Meinig, C.; Resing, J.; Delich, N. Hydroacoustics of a submarine eruption in the Northeast Lau Basin using an acoustic glider. In Proceedings of the OCEANS 2010 IEEE-Sydney, Sydney, Australia, 24–27 May 2010; pp. 1–6.
20. Berger, J.; Laske, G.; Babcock, J.; Orcutt, J. An ocean bottom seismic observatory with near real-time telemetry. *Earth Space Sci.* **2016**, *3*, 68–77. [[CrossRef](#)]

21. Miller, J.H.; Potty, G.R. *Modeling and Measuring Variability in 3-D Acoustic Normal Mode Propagation in Shallow Water Near Ocean Fronts Using Fixed and Moving Sources and Receivers*; ADA573346; Rhode Island University Narragansett Graduate School of Oceanography: Narragansett, RI, USA, 2007.
22. Liu, L.; Xiao, L.; Lan, S.-Q.; Liu, T.-T.; Song, G.-L. Using Petrel II Glider to Analyze Underwater Noise Spectrogram in the South China Sea. *Acoust. Aust.* **2018**, *46*, 151–158. [[CrossRef](#)]
23. Grigoli, F.; Cesca, S.; Rinaldi, A.; Manconi, A.; López-Comino, J.; Clinton, J.; Westaway, R.; Cauzzi, C.; Dahm, T.; Wiemer, S. The November 2017 Mw 5.5 Pohang earthquake: A possible case of induced seismicity in South Korea. *Science* **2018**, *360*, 1003–1006. [[CrossRef](#)] [[PubMed](#)]
24. Kim, K.-H.; Ree, J.-H.; Kim, Y.; Kim, S.; Kang, S.Y.; Seo, W. Assessing whether the 2017 Mw 5.4 Pohang earthquake in South Korea was an induced event. *Science* **2018**, *360*, 1007–1009. [[CrossRef](#)] [[PubMed](#)]
25. Merchant, N.D.; Barton, T.R.; Thompson, P.M.; Pirotta, E.; Dakin, D.T.; Dorocicz, J. Spectral probability density as a tool for ambient noise analysis. *J. Acoust. Soc. Am.* **2013**, *133*, EL262–EL267. [[CrossRef](#)] [[PubMed](#)]
26. Merchant, N.D.; Blondel, P.; Dakin, D.T.; Dorocicz, J. Averaging underwater noise levels for environmental assessment of shipping. *J. Acoust. Soc. Am.* **2012**, *132*, EL343–EL349. [[CrossRef](#)] [[PubMed](#)]
27. Alvarez, A.; Stoner, R.; Maguer, A. Performance of pumped and un-pumped CTDs in an underwater glider. In Proceedings of the 2013 OCEANS-San Diego, San Diego, CA, USA, 23–26 September 2013; pp. 1–5.
28. Robinson, S.P.; Lepper, P.A.; Hazelwood, R.A. *Good Practice Guide for Underwater Noise Measurement*; No.133; National Measurement Office: Teddington, UK, 2014; pp. 1–95.



© 2019 by the authors. Licensee MDPI, Basel, Switzerland. This article is an open access article distributed under the terms and conditions of the Creative Commons Attribution (CC BY) license (<http://creativecommons.org/licenses/by/4.0/>).